Nonlinear Time-Dependent Mechanical Behavior of Medium-Density Polyethylene Pipe Material

Suprio Das[1] and Ashutosh Sutra Dhar[2]

Abstract: Medium-density polyethylene (MDPE) pipes are extensively used for gas distribution systems in Canada and worldwide. MDPE pipe material possesses time-dependent mechanical properties that govern the performance of the pipes in service. In this research, an extensive laboratory investigation is carried out to investigate the time-dependent behavior of MDPE pipe material. Uniaxial tensile tests are conducted with samples (coupons) cut from the wall of a 60-mm diameter MDPE pipe. A tensile test with a sample of the full cross section of the pipe is also conducted to investigate the influence of sample type on the test results. The test program includes uniaxial testing at various strain rates ranging from $10^{-6}/\mathrm{s}$ to $10^{-2}/\mathrm{s}$ to capture the effects of loading rates, creep testing, and relaxation testing. The program revealed that the stress-strain responses of MDPE pipe material are highly nonlinear and strain rate-dependent. However, the strain rate effect is negligible below $10^{-6}/\mathrm{s}$, which is termed herein as the "reference strain rate." A numerical technique for modeling time-dependent behavior is proposed using the features available in a commercially available finite element software, Abaqus. In this technique, strain rate-dependent stress-strain models are used to simulate loading and unloading responses, and a power-law type creep-law model is used to simulate the creep/relaxation behavior. The proposed modeling approach successfully simulated the test results. **DOI: 10.1061/(ASCE)MT.1943-5533.0003695.**

Author keywords: Medium density polyethylene (MDPE); Gas distribution; Time-dependent behavior; Finite element modeling; Constitutive model.

Introduction

The use of polymer pipes has increased significantly over the last few decades due to their various advantages over metal pipes, including low cost, lightweight, ease of installation, and corrosion resistance. Water supply, cold water distribution, sewer, gas distribution, and irrigation are the major areas of application of polymer pipes. Medium-density polyethylene (MDPE) pipes are widely used for water and gas distribution systems. These buried distribution pipes are subjected to loads from the weight of the soil column above the pipe, the surcharge loads including live traffic and dead loads, internal pressure, and loads from ground movement resulting from landslides and seismic activities, if any. The behavior of the pipes under these loads is influenced by their interaction with the surrounding soil. Soil-pipe interaction analysis is generally performed to understand the behavior of pipes subjected to various loads. However, modeling of soil-pipe interaction for polyethylene pipes is complex because the behavior of polymer material is time-, temperature-, and strain rate-dependent. Polymer materials exhibit an instantaneous elastic response followed by viscoelastic (recoverable) and viscoplastic (irrecoverable) responses. Because the viscoelastic behavior initiates at a low-stress level, identifying a well-defined yielding point beyond which permanent strains develop is difficult.

Studies in the available literature on understanding the viscoelastic and/or viscoplastic behavior for MDPE pipe material are very limited. Hamouda et al. (2007) conducted uniaxial "tension-relaxation" tests using samples cut out from a thick-walled MDPE pipe. The tests conducted at two different strain rates revealed that MDPE behavior is highly nonlinear and strain rate-dependent. Liu et al. (2008) conducted creep tests with three different high-density polyethylene (HDPE) materials and MDPE pipe material. They revealed that the responses of polyethylene materials could be significantly different under loads due to differences in their molecular structures. Using the creep test results, they determined parameters for a multi-Kelvin type viscoelastic model for these materials. Bilgin et al. (2007) examined the thermal and mechanical properties of MDPE pipe material through stress relaxation tests and temperature ramp tests with full-scale pipe segments. They proposed constant relaxation modulus, instantaneous modulus, and stress relaxation rates, which are assumed to be independent of the applied strain rate. However, Hamouda et al. (2007) revealed that the relaxation behavior of the material could significantly depend on the applied strain rate. None of these studies extensively investigated the strain rate-dependent stress-strain relations and the relaxation/creep behavior of MDPE.

Several studies were conducted in the past to model the nonlinear time-dependent behavior of polyethylene pipe materials with attention to HDPE. Tobolosky (1960) used a convolution integral to simulate the viscoelastic behavior, which relates time-dependent stress with strain by a relaxation modulus. Popelar et al. (1990) expanded this method to include nonlinearity and temperature effects in stress relaxation behavior. Time-dependent relaxation moduli of HDPE pipe material were also developed as power-law relations with time (Chua and Lytton 1989; Hashash 1991). However, the time-dependent relaxation modulus can only be used to

[1]Graduate Student, Dept. of Civil Engineering, Memorial Univ. of Newfoundland, 1 Arctic Ave., St. John's, NL, Canada A1B 3X5. ORCID: https://orcid.org/0000-0003-3245-312X. Email: sdas@mun.ca

[2]Associate Professor, Dept. of Civil Engineering, Memorial Univ. of Newfoundland, 1 Arctic Ave., St. John's, NL, Canada A1B 3X5 (corresponding author). ORCID: https://orcid.org/0000-0001-5137-3921. Email: asdhar@mun.ca

Note. This manuscript was submitted on April 4, 2020; approved on September 28, 2020; published online on February 24, 2021. Discussion period open until July 24, 2021; separate discussions must be submitted for individual papers. This paper is part of the ***Journal of Materials in Civil Engineering***, © ASCE, ISSN 0899-1561.

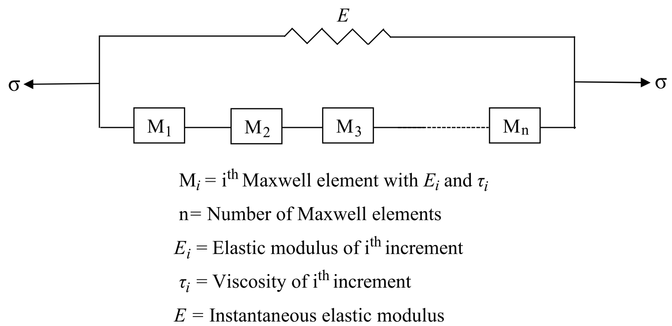

Fig. 1. Prony series model.

assess the responses at a particular strain level for which the power-law equation is developed. It cannot be used to evaluate the overall strain rate-dependent responses of the viscoelastic or viscoplastic material. Few other constitutive models were developed for polymer materials that overcome the limitations (Moore 1994; Zhang and Moore 1997; Chehab and Moore 2006; Suleiman and Coree 2004; Siddiquee and Dhar 2015; Hamouda et al. 2007). These models were used for finite element (FE) modeling of the time-dependent behavior of the materials. The major challenges with these models include (1) obtaining the model parameters from laboratory tests that would reasonably represent real behavior, and (2) the complexity of the models for implementation in commercially available FE codes. Viscoelastic models based on the Prony series are recently becoming popular due to their ease of implementation in FE codes (Bilgin 2014; Swain and Ghosh 2019). The Prony series is defined as an arrangement of several Maxwell elements in series with a parallel spring element, as indicated in Fig. 1. Bilgin (2014) used the built-in feature for the Prony series available in Abaqus version 5.8, which is commercially available FE softwar e, and successfully simulated the relaxation behavior of MDPE pipe material at very low strain levels (strain < 0.008). At the strain levels, the stress-strain response of the pipe material is almost linear. However, at higher strains (or stresses), the stress-strain response of the pipe material is nonlinear, which cannot be captured using the conventional Prony series. Bilgin (2014) obtained the model parameters from the relaxation test data of Bilgin et al. (2007). They did not investigate the creep and effects of the strain rate on the stress-strain responses.

The objectives of the current study are to experimentally investigate strain rate-dependent stress-strain behavior, relaxation behavior, and creep behavior of MDPE pipe material and to develop a numerical method to simulate the nonlinear time-dependent behavior. The motivation of this study is the need to model MDPE distribution pipes subjected to lateral ground movements. The pipelines are often subjected to lateral ground movements at various rates, causing strains in the axial directions of the pipes. However, the test results and a material model are currently not available for modeling of these pipes experiencing various ground movement scenarios. This study focuses on extending the database in the body of knowledge for MDPE pipe material, including the development of modeling techniques using commercially available FE software. The study includes (1) an experimental investigation of strain rate-dependent stress-strain behavior, relaxation behavior, and creep behavior using uniaxial tension tests. Tests with a complex loading history were also performed; (2) the development of rate-dependent constitutive relations for use in the FE modeling; and (3) the development of a FE modeling technique to simulate nonlinear time-dependent behavior. In the time-dependent modeling technique, strain rate-dependent stress-strain models are used to simulate loading and unloading behavior, and a power-law type creep-law model is used to simulate the creep/relaxation behavior. Although not used in this study, the models developed using the uniaxial tests can be applied for generalized models with multiaxial stress conditions using the von Mises theory (after Siddiquee and Dhar 2015; Chehab 2008). The proposed method is validated through a comparison with test results and the results from FE analysis using conventional Prony series.

Test Methods

Tensile tests were performed to investigate the time-dependent behavior (strain rate effect, creep, and relaxation) of MDPE pipe material commonly used in the Canadian gas distribution system (CSA B 137.4 certified). A test was first conducted on a whole pipe segment. Cholewa et al. (2011) indicated for a HDPE pipe that the stress-strain responses from whole pipe segment tests are different from those from coupon tests. The difference is attributed to the presence of residual stresses in the whole pipe resulting from the manufacturing process. However, the residual stress resulting from the manufacturing process is generally unknown, which may be different for pipes with different diameters. As a result, interpreting the results from a whole pipe segment test for the development of a constitutive model of the material is challenging. The residual stresses are released when the coupons are cut from the pipe wall. Thus, the coupon tests can be used to investigate the behavior of the pipe material, avoiding the influence of the residual stresses. Therefore, coupon tests were used in the present study. The whole pipe test was used to examine the extent of the impact of residual stresses on the pipe considered in this study.

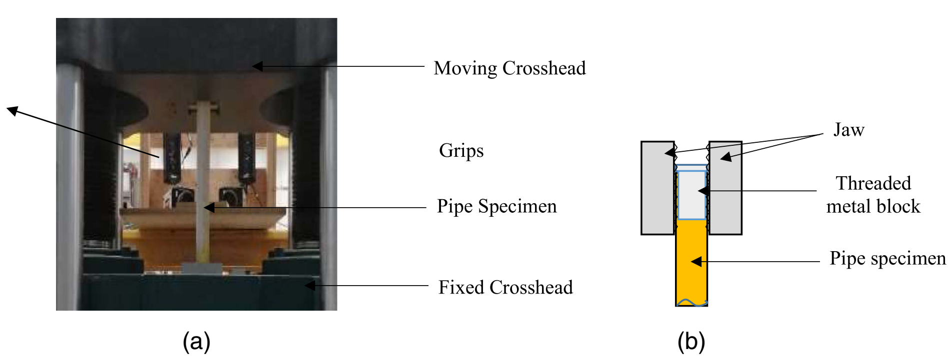

Fig. 2. Test set up and loading apparatus for full pipe test: (a) UTM machine; and (b) mechanism of grips.

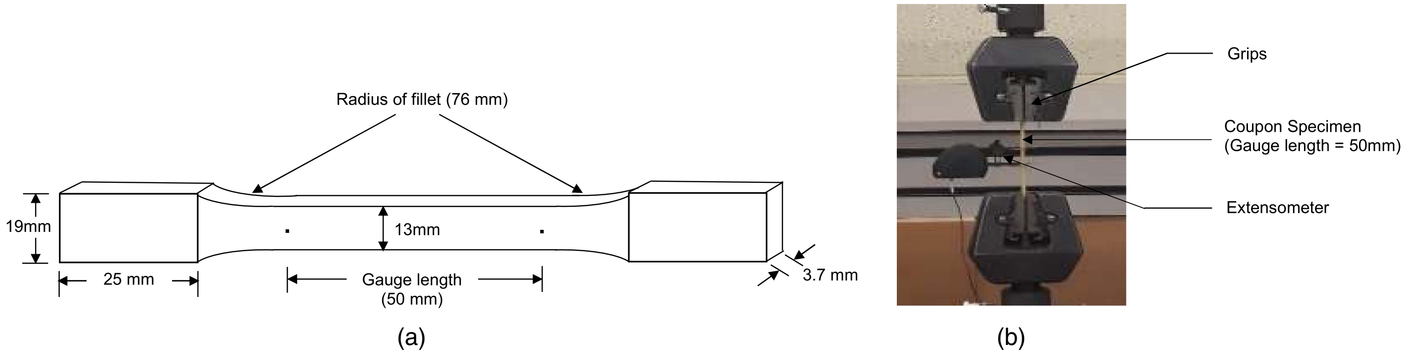

Fig. 3. Test set up and loading apparatus for coupon tests: (a) schematic of coupon specimen; and (b) tensile testing machine.

For the whole pipe test, a segment of a 42.2-mm diameter pipe was used with a gauge length of 500 mm. The pipe wall thickness is 4.5 mm. A special arrangement at the ends of the sample was made to apply axial tension using a universal testing machine (UTM) [Fig. 2(a)]. This arrangement included inserting a threaded metal block of a circular cross section at each end, well-fitted inside the pipe [Fig. 2(b)]. The metal blocks offer reactions against the gripping forces from the jaws of the UTM, allowing the jaws to firmly hold the pipe sample without it being lateral deflected. The load was applied to the sample using the vertical movement of the upper crosshead of the machine. The upward movement of the crosshead causes a tensile load, and downward movement causes a compressive load on the specimens. A load transducer, which was mounted in series with the specimen, measures the applied load and converts it into an electrical signal that an automated control system measures and displays. A change in the height of the specimen was measured by recording the ram position through the displacement transducer of the Instron machine (Norwood, Massachusetts), and the corresponding load was measured by a load cell. A computer-controlled system was used to monitor and record the outputs of the displacement transducer and the load cell.

For the coupon tests, the samples were prepared according to ASTM D638-14 specifications (ASTM 2003). A water jet was used to cut the pieces from the wall of 60.3-mm diameter MDPE pipes. A surface planer was then used to remove the curvature from the pieces. The length of the test specimens was parallel to the length of MDPE pipe. The coupon specimens were tested under uniaxial tension using an Instron (5585H) machine equipped with a load transducer (Fig. 3). A schematic of the samples is provided in Fig. 3(a). To measure strain in coupon specimens, Debnath and Dhar (2019) used uniaxial strain gauges at the center of the specimens for a cast iron pipe material. However, strain measurement using strain gauges was considered unsuitable for flexible MDPE coupons because the adhesive for gluing the strain gauges can stiffen the specimen surface, affecting the measured strains (Brachman et al. 2000). Therefore, strain within the gauge length was measured using a clip-on extensometer [Fig. 3(b)].

Tests were conducted under constant strain rates, creep at certain stress levels, and relaxation at certain strain levels. The machine's crosshead movements were used to control the displacement rate during the application of the load. Measured strains (using the extensometer) and the corresponding time intervals were then used to interpret the strain rates applied during the tests. The tests were managed, and data were obtained using a computer-controlled system equipped with Instron proprietary software. All tests were conducted at room temperature (22°C ± 1°C).

The same test was repeated two or three times to examine the repeatability of the test results. Table 1 indicates a summary of the test program undertaken. As indicated in the table, a total of 35 tests were conducted. Tests 1–21 are constant strain rate tests conducted at various strain rates, Tests 24–29 are relaxation tests, and Tests 30–35 are creep tests. Tests 22–23 were performed to examine the effect of loading history on stress-strain behavior. In Test 22, the strain rate was changed during the test. In Test 23, a loading-unloading-reloading cycle was applied.

Engineering stresses and strains were calculated based on the measured loads and elongations within the gauge length, respectively, for the interpretation of the test results. Engineering stresses and strains are conveniently used in practice and are, however, not significantly different from the corresponding true values at low strain levels typically encountered in buried pipelines (Cholewa et al. 2011).

Test Results

Constant Strain Rate Tests

Uniaxial tension tests were performed at constant strain rates ranging from a very small value to $10^{-2}/\mathrm{s}$. The very low strain rates are selected to identify the lower bound value below which the stress-strain response is independent of the strain rate. The existence of such a lower bound strain rate (termed "reference strain rate") is assumed in the development of an isotach-based viscoplastic model for HDPE pipe material (Siddiquee and Dhar 2015). However, this phenomenon has not been experimentally validated for MDPE pipe material. The test samples were loaded to strain beyond an "allowable strain limit" according to industry practice in Canada. An allowable strain limit of 8% has been adopted as an industry practice for MDPE pipes (Weerasekara and Rahman 2019). The tests were conducted to a strain of approximately 13%.

Fig. 4 indicates the mean stress-strain responses for different strain rates from the constant strain rate tests. The stress-strain responses from multiple tests for each strain-rate (Table 1) were found to be consistent with each other (maximum variation of less than 10% from the corresponding mean values). Therefore, the mean values presented in Fig. 4 are used to compare and validate the numerical models, which are subsequently discussed. Fig. 4 indicates that the stress-strain response of MDPE material is extensively strain rate-dependent, similar to HDPE pipe material reported in Zhang and Moore (1997). At any particular strain, the stress is higher for the tests conducted at a higher strain rate. The higher stress at the higher strain rate is associated with the overstress component of the total stress for viscous materials. According to the overstress theory (Perzyna 1966), the total stress in viscous materials can be decomposed into an equilibrium stress and

J. Mater. Civ. Eng., 2021, 33(5): 04021068

Table 1. Test program

Test number	Type of test	Remarks
1, 2, 3	Uniaxial tension test	Tests were conducted at 10^{-2}/s strain rate
4, 5, 6	Uniaxial tension test	Tests were conducted at 3×10^{-3}/s strain rate
7, 8, 9	Uniaxial tension test	Tests were conducted at 10^{-3}/s strain rate
10, 11, 12	Uniaxial tension test	Tests were conducted at 3×10^{-4}/s strain rate
13, 14, 15	Uniaxial tension test	Tests were conducted at 10^{-4}/s strain rate
16, 17	Uniaxial tension test	Tests were conducted at 10^{-5}/s strain rate
18, 19	Uniaxial tension test	Tests were conducted at 5.5×10^{-6}/s strain rate
20, 21	Uniaxial tension test	Tests were conducted at 10^{-6}/s strain rate
22	Strain rate change	Strain rate changed between 10^{-2}/s and 10^{-3}/s
23	Loading-unloading-reloading test	Loading-unloading-reloading test was conducted at 10^{-3}/s strain rate
24, 25	Relaxation test	Tests were conducted to 0.014 strain (initial strain rate: 10^{-3}/s)
26, 27	Relaxation test	Tests were conducted to 0.024 strain (initial strain rate: 10^{-2}/s)
28, 29	Relaxation test	Tests were conducted to 0.052 strain (initial strain rate: 10^{-2}/s)
30, 31	Creep test	Tests were conducted to 2 MPa (initial strain rate: 10^{-4}/s)
32, 33	Creep test	Tests were conducted to 8.5 MPa (initial strain rate: 10^{-3}/s)
34, 35	Creep test	Tests were conducted to 10 MPa (initial strain rate: 10^{-2}/s)

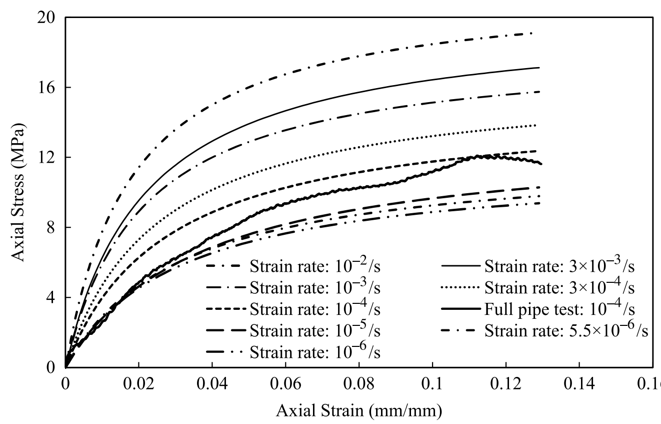

Fig. 4. Rate dependent stress-strain responses from constant strain-rate tests (mean values).

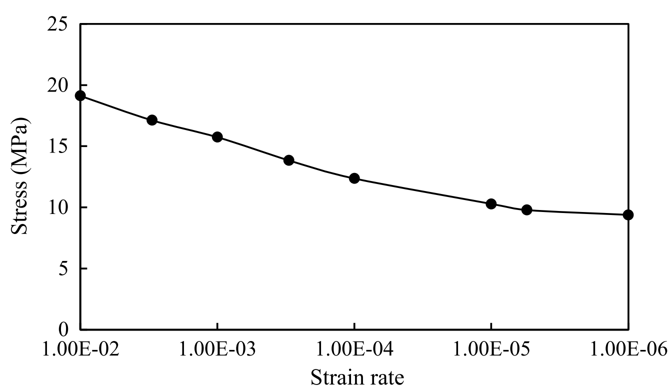

Fig. 5. Effect of strain rate on stresses of MDPE.

an overstress. The equilibrium component is independent of the strain rate (i.e., inviscid stress), whereas the overstress component is strain rate-dependent (i.e., viscous stress). The equilibrium stress-strain relation of materials corresponds to a test conducted at the infinitely slow strain rate. Siddiquee and Dhar (2015) defined a very slow strain rate for HDPE as the "reference strain rate" below

Table 2. Initial modulus of MDPE at various strain rates

Strain rate (/s)	Initial modulus, E_{ini} (MPa)
10^{-2}	1,064
3×10^{-3}	902
10^{-3}	776
3×10^{-4}	658
10^{-4}	566
10^{-5}	413
5.5×10^{-6}	337
10^{-6}	325

which the strain-rate dependence of the stress-strain relation is practically insignificant. The overstresses are then calculated from the total stress-strain response by subtracting the stress-strain response at the reference strain rate. To examine the "reference strain rate" for MDPE, the measured stresses at a particular strain (i.e., 0.13) are plotted against the strain rates in Fig. 5, which indicates that the stress initially decreases with a decrease in strain rate. The line is almost horizontal between strain rates of 5.5×10^{-6}/s and 10^{-6}/s, indicating an insignificant influence of the strain rate on stress. Thus, the strain rate of 10^{-6}/s can be taken as the reference strain rate for MDPE pipe material.

Fig. 4 indicates high nonlinearity in the stress-strain responses for MDPE pipe material. However, at very small strains (strain < 0.01), the responses are almost linear. Bilgin et al. (2007) also observed close to linear stress-strain relations at lower strain levels (strains < 0.008) for MDPE pipe material. They calculated the instantaneous modulus of elasticity (initial tangent modulus) of 958 MPa at room temperature (21°C), which is within the reported values in the literature (Bilgin et al. 2007). Note that the strain rate effect was not accounted for in the initial moduli reported in the literature and in Bilgin et al. (2007). However, as seen in Fig. 4, the initial modulus significantly depends on the strain-rates. Initial tangent moduli calculated at various strain rates from the test results are presented in Table 2. The table includes the results of two additional preliminary tests conducted at strain rates of 3×10^{-3}/s and 3×10^{-4}/s prior to the execution of the test program. In Table 2, the initial modulus is found to range from 325 MPa to over 1,000 MPa, depending on the rate of strain. According to the values indicated in the table, the initial moduli reported in the

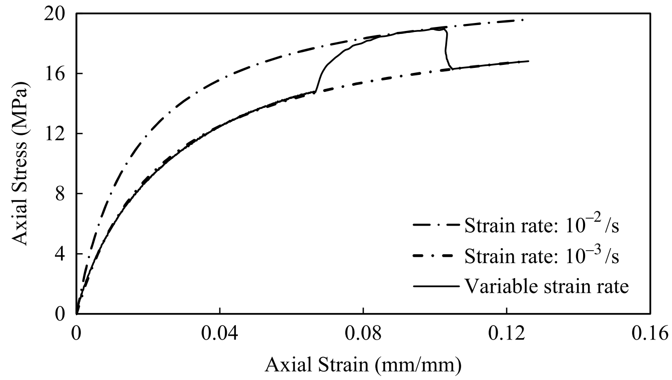

Fig. 6. Experimental results for strain-rate-change test.

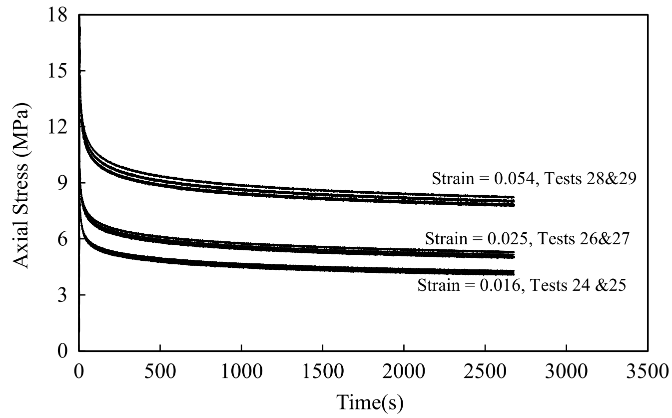

Fig. 8. Experimental results for relaxation tests (in-between lines represent mean values).

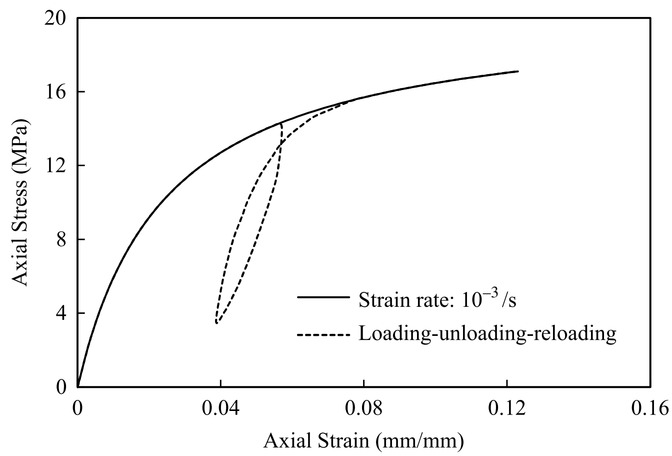

Fig. 7. Experimental results for loading-unloading-reloading test.

literature (i.e., ~958 MPa, Bilgin et al. 2007) corresponds to the values at a strain rate of 10^{-3}/s to 10^{-2}/s.

The stress-strain response obtained from the full pipe test is also included in Fig. 4. A strain rate of 10^{-4}/s was applied for the test with a full pipe segment. In this test, the stress is initially underestimated, which is due to the slipping of the grips. However, at a higher load, it matches the coupon test results conducted at a similar strain rate (10^{-4}/s). Thus, the influence of residual stress is insignificant for the pipe, and the coupon test results reasonably represent the mechanical behavior of the pipe material.

In Test 22, a strain rate of 10^{-3}/s was applied up to a strain of 0.065. At 0.065 strain, the rate was changed from 10^{-3}/s to 10^{-2}/s that continued until a strain of 0.11. Then, the strain rate was changed back to 10^{-3}/s. The results are indicated in Fig. 6, along with the stress-strain responses corresponding to the strain rates of 10^{-3}/s and 10^{-2}/s, respectively. As seen in the figure, for changing the strain rate from 10^{-3}/s to 10^{-2}/s, an increase of stress occurred. The stress-strain curve then matches with the stress-strain response corresponding to the strain rate of 10^{-2}/s. Similarly, when the strain rate was changed back to 10^{-3}/s, the response follows the stress-strain response corresponding to 10^{-3}/s strain rate with a sudden drop. This indicates that the stress-strain responses of MDPE material depend predominantly on the strain-rate, which is not affected by the loading history. Similar responses were reported earlier for HDPE in Zhang and Moore (1997).

Fig. 7 indicates the results of the loading-unloading-reloading test. The test was conducted at the same strain rate of 10^{-3}/s during the load-unload-reload cycle. This figure reveals that the unloading and reloading do not affect the strain rate-dependent stress-strain response beyond the previous stress level. As a result, the stress-strain curve for reloading gradually approached the monotonic loading curve corresponding to the strain rate.

Relaxation and Creep Tests

Stress relaxation and creep tests were conducted to examine the viscous behavior of MDPE pipe material. To conduct a relaxation test, a specimen is tensioned at a constant strain rate to a predetermined strain. The strain is then held constant for the rest of the test. Fig. 8 indicates the results of the stress relaxation tests conducted. Each test was performed twice to examine the repeatability. In Tests 24 and 25, an initial strain rate of 10^{-3}/s was applied up to a strain of ~0.016, and the strain was then held constant. In Tests 26 and 27, an initial strain rate of 10^{-2}/s was applied up to a strain of 0.025. In Tests 28 and 29, an initial strain rate of 10^{-2}/s was applied up to a strain of 0.053, when the strain was held constant. The average maximum stresses at the three sets of tests were 9.2, 12.8, and 17.8 MPa, respectively. As observed in Fig. 8, each pair of relaxation tests for a particular strain level are consistent with each other, confirming the repeatability of the test results. Therefore, the average responses are used for further interpretations.

Fig. 8 indicates that MDPE pipe material exhibits typical relaxation behavior with a high initial decrease of stress that stabilizes after a period. The relaxation behavior is expected to stop when the stress reaches the equilibrium (inviscid) stress-strain relation (i.e., reference stress-strain relation), and the overstress becomes zero (Colak and Dusunceli 2006). The stress-strain responses during the relaxation tests are compared with the reference stress-strain relation (at the strain rate of 10^{-6}/s) in Fig. 9. These responses reveal that the stress is reduced at constant strains during relaxation and finally stops at the minimum values corresponding to the reference (equilibrium) stress-strain relations. This observation confirms the existence of the reference stress-strain responses at the strain rate of 10^{-6}/s for MDPE pipe material.

In the creep tests, the specimens were subjected to tension at constant rates and deformed to the predetermined load levels. The load is then kept constant for the rest of the test duration. Fig. 10 indicates the results of the creep tests conducted. In Tests 30 and 31, an initial strain rate of 10^{-4}/s was applied up to 2 MPa

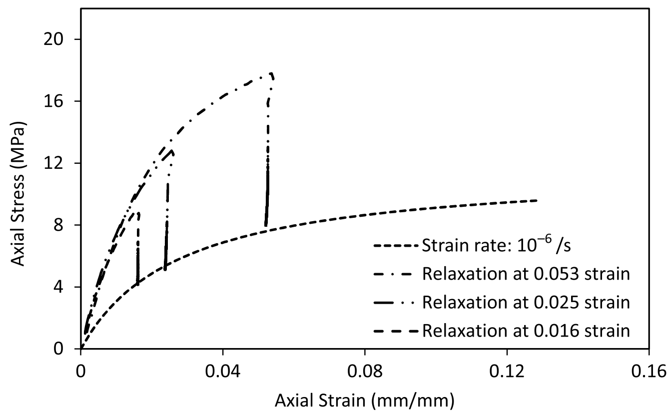

Fig. 9. Stress-strain responses of relaxation tests.

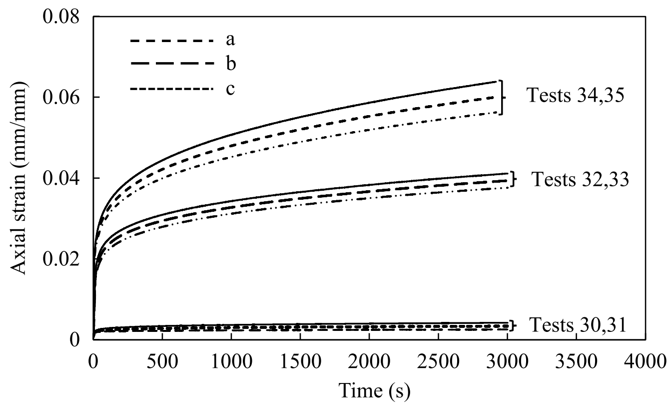

Fig. 10. Experimental results of creep tests (a, b, and c are mean values).

of stress. In Tests 32 and 33, an initial strain rate of 10^{-3}/s was applied up to 8.5 MPa of stress, and in Tests 34 and 35, an initial strain rate of 10^{-2}/s was applied up to 10 MPa of stress. The initial strains corresponding to the applied stress levels are 0.021, 0.025, and 0.052 in the tests conducted with strain rates of 10^{-4}/s, 10^{-3}/s, and 10^{-2}/s, respectively. Fig. 10 indicates that only primary and secondary creep exist over the test durations. During the primary creep stage, the increase in the creep strain is relatively high over time, whereas during the secondary creep stage, the creep strain rate is almost constant. No tertiary creep was observed within the test duration, even for the highest stress levels considered.

Modeling Time-Dependent Behavior

Different constitutive models were developed in the past to capture the time-dependent behavior of HDPE materials (Chua and Lytton 1989; Zhang and Moore 1997; Chehab and Moore 2006; Suleiman and Coree 2004; Siddiquee and Dhar 2015). However, models for MDPE pipe material are very limited. A constitutive model adaptable to the framework of a widely used finite element (FE) model is required to assess the performance of the pipe structure using FE analysis. A framework for modeling the time-dependent behavior of MDPE pipe material is developed using the features available in the commercially available FE software, Abaqus, version 6.14 (Dassault Systemes 2015).

In Abaqus, two features are available for modeling the viscous behavior of material—Prony series and Creep law. Both features are employed to simulate the experimental results.

Prony Series

The Prony series is a simplistic form of modeling the viscous effect of viscoelastic material (Powel 1983). This model is based on the linear viscoelastic theory, in which the elastic and viscous components are modeled as combinations of springs and dashpots. Here, the spring is considered the linear-elastic component and is represented using the following stress (σ)-strain (ε) relation:

$$\sigma = E\varepsilon \tag{1}$$

where E = elastic modulus (spring constant).

The dashpot is considered the viscous component. Its stress depends on the strain rate and is given as follows:

$$\sigma = \eta \frac{\delta\varepsilon}{\delta t} \tag{2}$$

where η = viscosity constant. Linear viscoelastic constitutive models are constructed by the superposition of these components. Because the response of the dashpot is time-dependent, the behavior of a viscoelastic material that is modeled by a parallel and/or series combination of springs and dashpots is also time-dependent.

The most general form of the linear model for viscoelasticity is known as the generalized Maxwell model. This model consists of "n" spring-dashpot Maxwell elements arranged in series. The Prony series is based on the generalized Maxwell model with the addition of a parallel spring element (Fig. 1). The Prony series expansion for the relaxation modulus (G) of the material can be expressed as follows (Dassault Systemes 2013):

$$G(t) = G_0\left\{1 - \sum_{i=1}^{N} g_i(1 - e^{-t/\tau_i})\right\} \tag{3}$$

where $G(t)$ = modulus at time t; G_0 = instantaneous modulus (corresponding to the parallel spring element); g_i = normalized modulus (G_i/G_0) of the ith Maxwell element; and τ_i = retardation time constant of the ith element, defined as η_i/G_0.

In Abaqus, several Maxwell elements are used in parallel to a spring element to simulate the available data. The parameters of the Prony series model in Abaqus can be defined using one of the following three options: (1) direct specification of Prony series parameters, (2) inclusion of relaxation test data, and (3) inclusion of creep test data. Prony series parameters, including the number of Maxwell elements, are automatically calculated using the relaxation or creep data in options (2) and (3). Relaxation data are provided as a normalized relaxation modulus (g_t), and creep data are provided as normalized compliance (C_t), which are calculated by dividing the corresponding data by their initial value. Because the strain is constant, the normalized values of the relaxation modulus (the ratio of the output stress to the input constant strain) is the same as the ratio of stress, $\sigma(t)$, to the initial stress. Similarly, the normalized value of compliance (the ratio of output strain to the input constant stress) can be obtained by dividing the strain, $\varepsilon(t)$, by its initial value. In the current study, both the creep test and relaxation test data obtained from the laboratory tests are used. The normalized relaxation moduli calculated for each of the three relaxation tests are indicated in Fig. 11. The average values from these three curves were implemented in Abaqus to calculate the Prony series parameters. Table 3 indicates the Prony series parameter obtained using the relaxation test data. Normalized modulus and retardation times for three

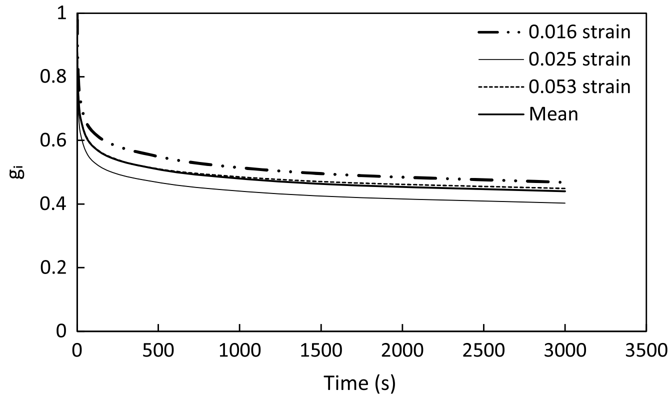

Fig. 11. Variation of normalized relaxation modulus g_i with time from relaxation tests.

Table 3. Prony series parameter obtained from relaxation test

i	g_i	τ_i
1	0.0796	0.14397
2	0.18199	3.9036
3	0.16192	43.873
4	0.13642	789.72

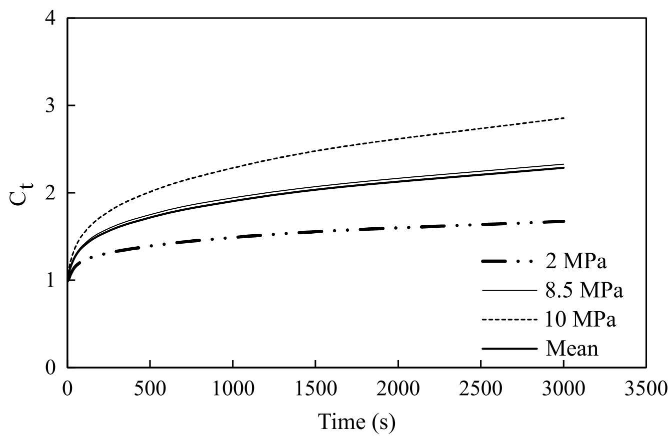

Fig. 12. Variation of normalized compliance C_t with time from creep tests.

Table 4. Prony series parameters obtained from creep tests

i	g_i	τ_i
1	0.27382	34.754
2	0.28876	634.90

Maxwell elements are obtained from Abaqus (Table 3). Similarly, the average normalized compliance calculated from creep test results was used in Abaqus to calculate the Prony series parameter. Fig. 12 indicates the normalized compliance calculated using creep test results. Table 4 indicates the Prony series parameters obtained using the data. Parameters for two Maxwell elements are obtained, as presented in the table. Thus, Prony series parameters from relaxation test data (Table 3) are different from those from the creep test data (Table 4). The effects of these different sets of parameters on the modeling of the time-dependent behavior are examined through the simulation of the test results, as subsequently discussed in this paper.

Table 5. Creep law parameters for creep tests

Maximum stress (MPa)	A	n	m
2	3×10^{-11}	1.825	−0.7
8.5	3×10^{-11}	1.87	−0.7
10	3×10^{-11}	1.89	−0.7

Creep Law

Creep law is another feature available in Abaqus for modeling the viscous behavior of viscoelastic material. The main advantage of this model over the Prony series is that it can simultaneously consider both plasticity and viscous behavior. In Abaqus, creep behavior can be defined using the user subroutine "creep" or by providing creep law parameters as input. Two common creep laws are available: the power law and the hyperbolic-sine law. Among them, the power law creep model is the simplest but is not applicable for simulation near crack tips where creep strain rates frequently indicate an exponential dependence on stress. The power law creep model is considered in the current study.

The power law model has two versions: the time-hardening version and the strain-hardening version. The time hardening version is applicable when the stress state remains essentially constant, and the latter is applicable when the stress state varies during the analysis. In this study, a time-hardening version of the power law creep model has been used to simulate creep when the stress state is constant. The equation of the time hardening form of the model is as follows [Eq. (4)]:

$$\dot{\varepsilon}_c = A\tilde{q}^n t^m \quad (4)$$

where $\dot{\varepsilon}_c$ = creep strain rate; $\tilde{q}$ = deviatoric stress; t = total time; and A, n, and m are the power law constants. Eq. (4) is the rate formulation of the Norton-Bailey creep law, which is mostly applicable in the primary creep regime (May et al. 2013). The constants of the equation can be determined from curve fitting with the creep and relaxation test data. Table 5 indicates the parameters obtained through fitting with creep test data. Because viscoelasticity and viscoplasticity in polymer generally occur during the deviatoric deformations (Pulungan et al. 2018; Siddiquee and Dhar 2015), the deviatoric component is considered for the determination of parameters. The number of Prony series terms required to match with the test data is automatically obtained from Abaqus through iterations. As seen in Table 5, "A" and "m" are the same for each stress level, whereas "n" increases with the increment of the stress level. The variation in "n" with maximum applied stress is plotted in Fig. 13. Similarly, parameters obtained for the relaxation tests are indicated in Table 6, where "A" and "m" are constant. However, "n" decreases with an increase in strain levels. The variation in "n" with maximum applied strain is plotted in Fig. 14. The change in "n" with an increase in stress or strain is almost linear for the ranges of stresses and strains observed.

Proposed Modeling Framework

Different approaches were employed in modeling the time-dependent behavior of polymer materials, including the empirical

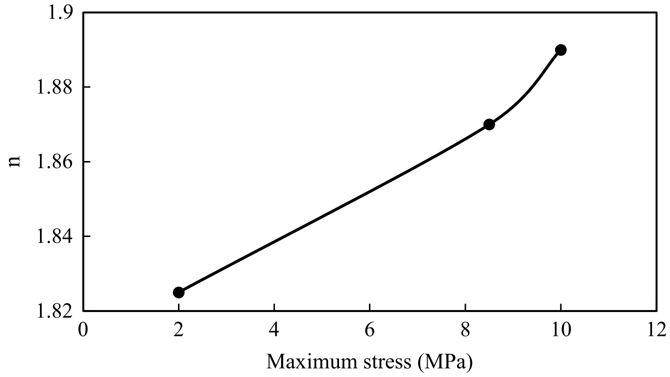

Fig. 13. Creep law parameter "n" from creep test data.

Table 6. Creep law parameters for relaxation tests

Maximum strain (mm/mm)	A	n	m
0.014	3×10^{-11}	1.915	−0.92
0.024	3×10^{-11}	1.875	−0.92
0.052	3×10^{-11}	1.815	−0.92

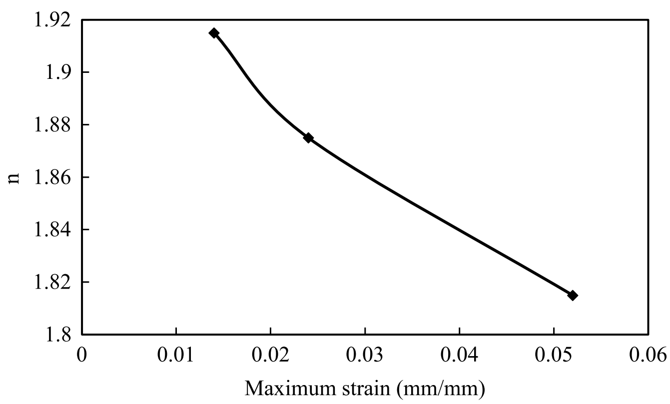

Fig. 14. Creep law parameter "n" from relaxation test data.

models developed through the fitting with the experimental data (Suleiman and Coree 2004), rheological models using springs and dashpots (Chehab and Moore 2006; Bilgin 2014), and the overstress theory (Colak and Dusunceli 2006; Siddiquee and Dhar 2015). The models are sometimes too complex for implementation in FE analysis using available software. Among these, the empirical models are relatively simple and can provide practical solutions using only a few fitting parameters. Empirical models proposed can be implemented using the features available in Abaqus.

The tests conducted in this study reveal that the stress-strain behavior of MDPE pipe material is highly nonlinear and strain rate-dependent. To account for the nonlinear strain rate-dependent stress-strain relation, creep, and relaxation, the following approach is proposed.

1. Nonlinear strain rate-dependent stress-strain relations are developed from experimental data and are provided as input to the FE model. The appropriate constitutive model from the input relations is then used in the analysis based on instantaneous strain rates calculated at a time step (subsequently discussed in more detail).
2. The creep law [Eq. (4)], which is available in Abaqus, is used to simulate the relaxation and creep. In Abaqus, the creep strain rate calculated using Eq. (4) is used to calculate the strain increment ($\Delta\varepsilon$) for any time increment (Δt). This incremental strain is added to the total strain obtained from the previous time step for the simulation of creep (when the stress is constant). Because the total strain is constant during relaxation, the elastic component of the strain is reduced by $\Delta\varepsilon$ (the creep strain increment). Thus, the stress calculated from the elastic strain is reduced.

The proposed modeling approach is implemented in Abaqus using its USDFLD feature.

Nonlinear Strain Rate-Dependent Stress-Strain Relations

The hyperbolic model is one of the simplest approaches to model nonlinearity. Kondner (1963) and Duncan and Chang (1970) introduced a simplified hyperbolic model to characterize the time-dependent nonlinear response of the soil. The general equation of the hyperbolic model is given as follows [Eq. (5)]:

$$\sigma = \frac{\varepsilon}{m + n\varepsilon} \tag{5}$$

where "m" and "n" are the constants to be estimated through nonlinear regression analysis with the test results.

Considering the strain rate-dependent behavior of polymer materials, Suleiman and Coree (2004) proposed a modification to the hyperbolic model for HDPE pipe material as follows:

$$\sigma = E_{ini}\left(\frac{\varepsilon}{1 + \eta\varepsilon}\right) \tag{6}$$

where E_{ini} is the initial modulus; and η is a hyperbolic constant. The parameters are strain rate-dependent and can be obtained using the following equations (Suleiman and Coree 2004):

$$E_{ini} = a(\dot{\varepsilon})^b \tag{7}$$

$$\eta = \frac{a(\dot{\varepsilon})^b}{c + d\ln(\dot{\varepsilon})} \tag{8}$$

where $\dot{\varepsilon}$ = strain rate; and a, b, c, and d are constants that can be determined by fitting with the stress-strain responses obtained from uniaxial tension or compression tests.

As previously stated, MDPE pipe material exhibits highly nonlinear and strain rate-dependent material behavior. Therefore, the model proposed in Suleiman and Coree (2004) is employed to represent the nonlinear stress-strain relations. Model parameters are determined based on the strain rate-dependent stress-strain relations obtained from the uniaxial tensile tests previously discussed. The parameters calculated from the curve fitting are indicated in Table 7. Fig. 15 compares the test results with the stress-strain relations obtained from the hyperbolic model with the parameters in Table 7, revealing that the developed hyperbolic model reasonably predicts the experimental stress-strain relations. The stress-strain response corresponding to the reference strain rate is independent of the strain rate. Therefore, Eq. (6) with a strain-rate independent initial modulus and hyperbolic constant (corresponding to the test data for a strain-rate of 10^{-6}/s) is used to model the stress-strain response at and below the reference strain rate (10^{-6}/s).

Table 7. Parameters for hyperbolic model

Hyperbolic parameters	Values
a	2,000
b	0.137
c	27.5
d	1.29

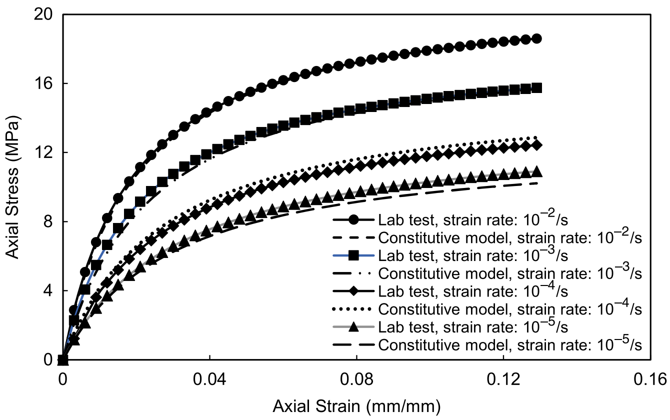

Fig. 15. Comparison of mean test results with hyperbolic model.

Implementation in Abaqus

In Abaqus, the elastic modulus, E (initial slope of the stress-strain curve), and the nonlinear part of the stress-strain relation can be provided as separate inputs. The nonlinear part is obtained from the total stress-strain relation [e.g., Eq. (6)] by subtracting the linear component of the strain calculated as σ/E. Each of the inputs can also be defined against field variables. In the current study, the strain rate is employed as the variable to allow the appropriate stress-strain relation to be used based on the magnitude of the strain rate. The strain rate is calculated and communicated with the main part of the analysis in Abaqus using the user subroutine USDFLD (after Muntakim et al. 2018). The USDFLD allows field variables at a material point to be defined as a function of time or solution-dependent parameters. It provides access to material point quantities at the start of a time-step increment and provides an explicit solution. In this process, the material properties are not influenced by the results obtained during the increment. Thus, the accuracy of the solution depends on the size of the time increment used, which can be controlled by the variable PNEWDT (Dassault Systemes 2015). At the start of the increment, a utility routine, GETVRM, is used to access the material point. By calling GETVRM with the appropriate output variable keys, the values of the material point quantities are obtained. The variables ARRAY, JARRAY, and FLGRAY are used to recover the values of the material point data (the floating-point, integer, and character data). At each increment, the field variables are restored to the values interpolated from the nodal values and introduced with the user-defined state variable STATEV, which can be recalled using the variable key "SDV" in the GETVRM utility routine.

In this study, GETVRM is used to access all strain components. The user-defined state variables are assigned to store the current strain component, time increment, and calculated strain rate for use in subsequent time steps. The strain rate is calculated based

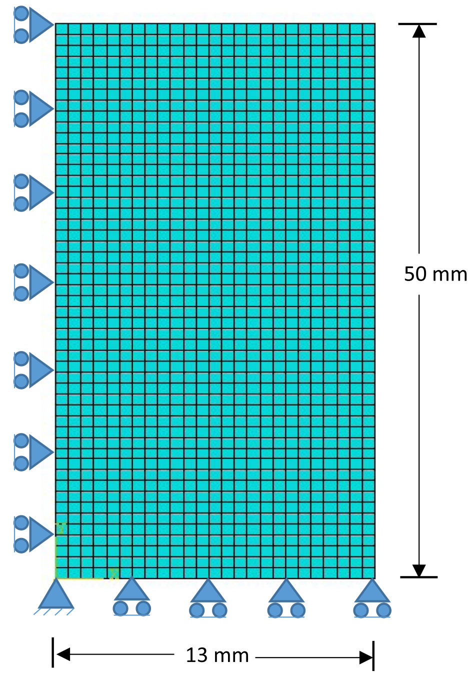

Fig. 16. FE model.

on the current strain (accessed by the GETVRM), the previous strain (stored in user-defined variables), and the time increment (accessed by USDFLD).

The variable, FIELD, which is an array containing field variables at the current material point, is used to assign the strain rate. Using the information of the FIELD variables given in the input file, Abaqus calculates the material parameters from the given strain rate-dependent stress-strain models.

Along with USDFLD previously discussed, the creep law features are included to account for the creep and relaxation effects. The creep law parameters obtained from creep tests are given in the Abaqus input file.

Validation of the Modeling Approach

Finite element analysis was performed to simulate the test results using the proposed method for validation. As previously discussed, tension tests were conducted using coupon specimens of 13-mm width (width of the narrow section) and 50-mm gauge length. The tests were performed using the application of constant strain rates ranging from 10^{-6}/s to 10^{-2}/s. These strain rate-dependent stress-strain relations were simulated with FE modeling using Abaqus. Fig. 16 indicates the FE mesh used in the analysis. The same size of the specimen was modeled. Smooth rigid boundaries were used at the bottom and the left side. The horizontal and vertical translations were restrained at the corner node to ensure stability. At the top of the mesh, a uniform deformation was applied at the same rates as those applied during the tests.

Simulation of Uniaxial Tension Tests

The results of the FE simulation of the uniaxial tension tests are compared with test results in Fig. 17. The stress-strain relations obtained using the proposed method are compared in Fig. 17(a), in which a reasonable agreement between the simulated and experimental results is observed. Thus, the method employed is capable

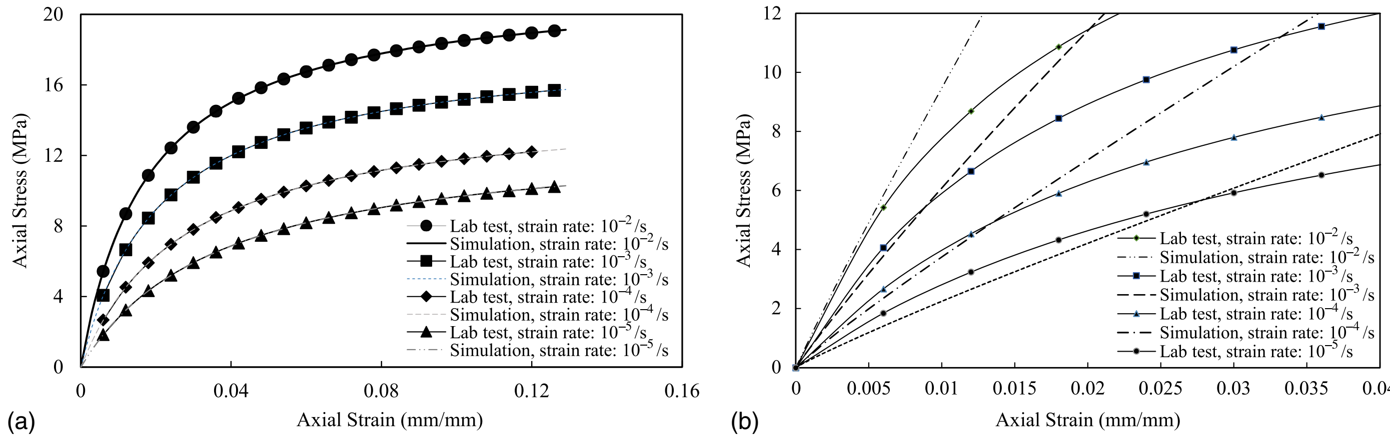

Fig. 17. Finite element simulations of uniaxial tension tests: (a) proposed model; and (b) Prony series.

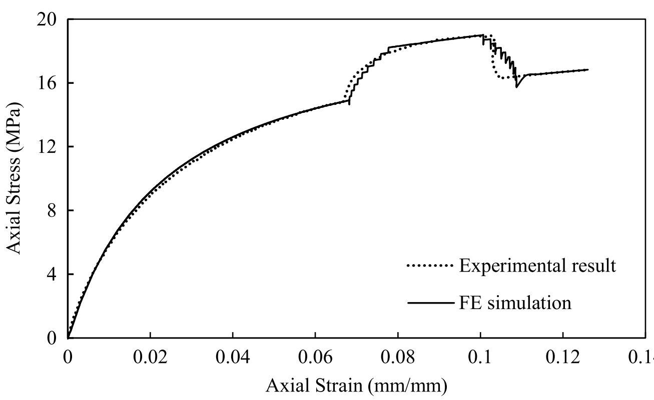

Fig. 18. Simulation of strain-rate-change test.

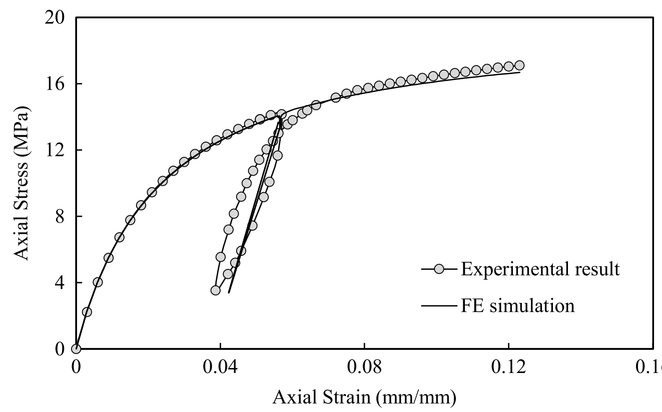

Fig. 19. Simulation of loading-unloading-reloading test.

of predicting the rate-dependent stress-strain behavior of MDPE material. Fig. 17(b) compares the test result with the results of the simulation using the conventional Prony series. The conventional Prony series appears to be only applicable at very low strain (less than 1%), for which the stress-strain response is linear. During the Prony series simulation, instantaneous elastic modulus and mean normalized relaxation modulus (g_t) obtained from the relaxation tests were used. Because the Prony series approach cannot account for the nonlinearity of the material, the nonlinear stress-strain relations observed at higher strain cannot be successfully simulated.

A strain rate change test performed during the experimental tests is also successfully simulated by the proposed method of analysis. During the experiment, the strain rate was changed from 10^{-3}/s to 10^{-2}/s at an axial strain of 0.065 (mm/mm) and then back to 10^{-3}/s at an axial strain of 0.11 (mm/mm). Fig. 18 provides a comparison of the simulated and experimental results of this test and indicates that the proposed technique reasonably predicted the experimental behavior during the change in the strain rate. Numerical noises exist in the results of the simulation during the changes in the strain rates. To minimize the noise, a control was applied to the strain increment using the USDFLD. The maximum strain increment of less than 15% was found to reduce the noise to a reasonable level.

The proposed method also reasonably predicted the loading-unloading-reloading response observed in the tests. Fig. 19 compares the FE simulation and experimental results and indicates that the observed loading-unloading-reloading behavior matches with the FE simulation. However, the hysteresis loop during the unloading-reloading cycle is not successfully simulated.

Simulation of Creep and Relaxation Tests

During the creep and relaxation tests, the specimen is first loaded with certain strain rates to the desired stress and strain level, respectively. This loading path can be simulated using the proposed strain rate-dependent stress-strain model. The creep and relaxation processes can then be simulated using the proposed creep law model. The Prony series can also be used to simulate the creep and relaxation behavior. In this case, secant modulus can be used to reach the desired level of stress and strain. The nonlinear loading path cannot be simulated using the conventional Prony series model. The creep and relaxation behaviors are simulated using the proposed modeling approach and conventional Prony series. In Fig. 20, the simulation creep behavior results are compared with the test results, indicating that the proposed model can reasonably predict the creep behavior observed during the tests [Fig. 20(a)]. The Prony series with parameters obtained from both creep and relaxation tests were employed. Fig. 20(b) indicates that both creep and relaxation test-based parameters can calculate the creep behavior to some extent. The creep test-based parameters provided a better prediction of the creep behavior, as expected.

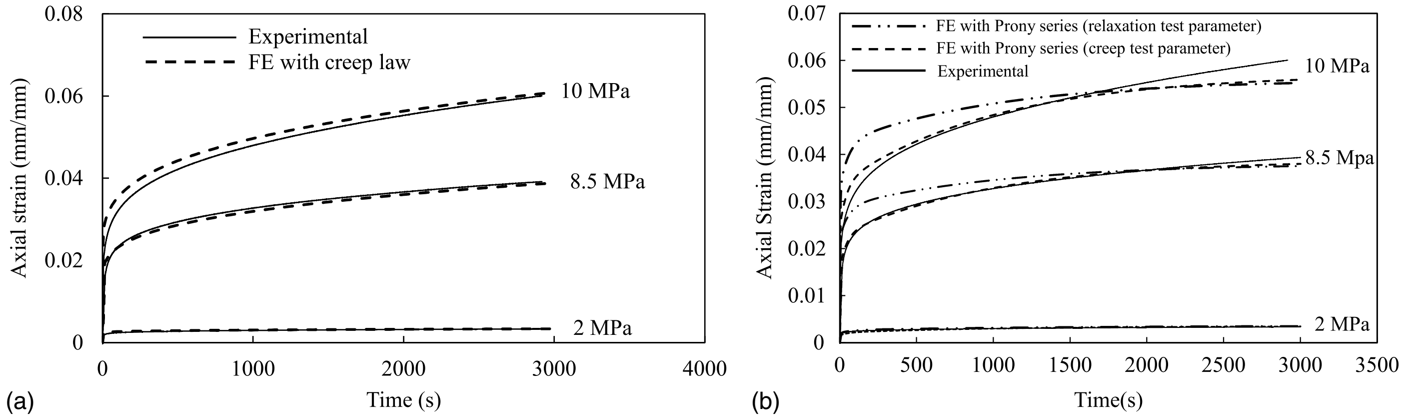

Fig. 20. Simulation for creep tests: (a) proposed model; and (b) Prony series.

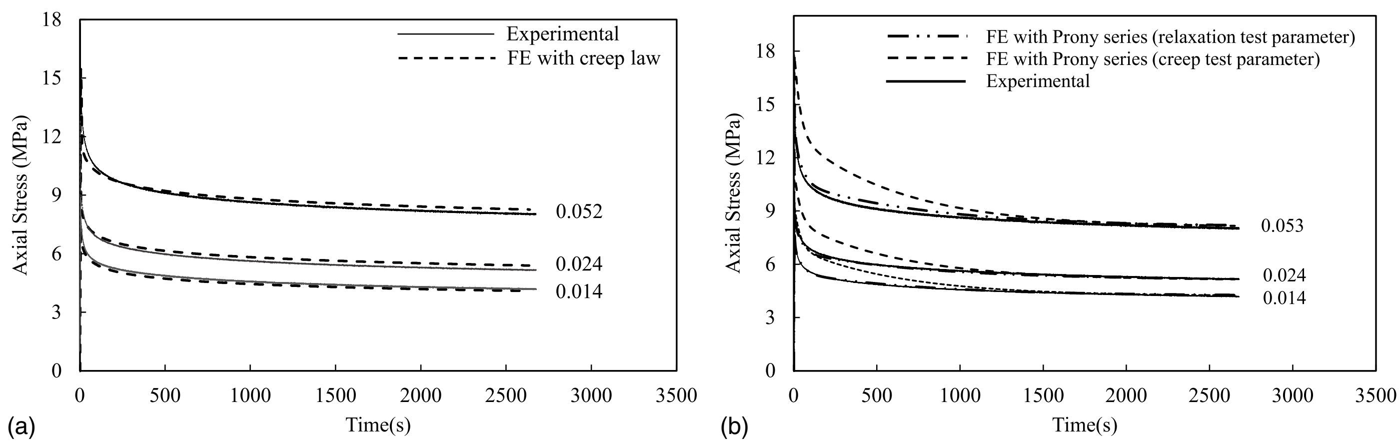

Fig. 21. Simulation for relaxation tests: (a) proposed model; and (b) Prony series.

The discrepancies in the simulation from the tests results are observed in Fig. 20(b), which is attributed to the nonlinearity of the material behavior that could not be captured using the Prony series. However, the proposed modeling approach can be used to account for the nonlinearity.

Similar results are obtained from a comparison of the relaxation test results (Fig. 21). The proposed modeling approach reasonably simulates the relaxation behavior [Fig. 21(a)], whereas the Prony series model overpredicts the stresses when creep-based parameters are used. However, the Prony series method reasonably simulated the relaxation test results with parameters based on the relaxation test data.

The Prony series approach is applicable to simulate linear viscoelastic responses and, thus, is not suitable for large strain when the stress-strain responses are nonlinear. The proposed modeling technique can be applied to simulate the nonlinear viscous response of MDPE pipe material. In this case, the creep law model can be used to simulate the creep and relaxation behavior.

Conclusions

The time-dependent nonlinear behavior of MDPE material is systematically investigated using laboratory tests and numerical methods. The major findings from this research are as follows.

1. The stress-strain responses of MDPE pipe material are highly nonlinear and strain rate-dependent. However, these can be approximated as linear at a very small strain.
2. The stress-strain response can be approximated to be independent of the strain rate at a strain rate at or below $10^{-6/s}$. This strain rate of $10^{-6/s}$ can be termed as the "reference strain rate" for isotach-based modeling.
3. Initial values of the modulus of elasticity are strain rate-dependent. For a strain of $10^{-6/s}$ to $10^{-2/s}$, the initial modulus ranged from 325 to 1,054 MPa.
4. A hyperbolic constitutive model was developed for MDPE pipe material at various strain rates that can simulate the nonlinear rate-dependent stress-strain behavior.
5. A new modeling technique is proposed for FE modeling of nonlinear strain rate-dependent material behavior of MDPE pipe material using Abaqus. The modeling approach can successfully simulate the strain rate-dependent stress-strain response observed in laboratory tests. The approach also reasonably simulates the loading-unloading-reloading response and a change in the strain rate.
6. The Prony series approach is only applicable for linear viscoelastic material. To account for the nonlinear responses, the creep law model is implemented in the proposed framework. The proposed creep law model successfully simulates the observed creep and relaxation behavior.

J. Mater. Civ. Eng., 2021, 33(5): 04021068

7. The creep law model involves three parameters (A, n, m). The magnitude of "A" and "m" are found to be independent of applied stress and strain levels, whereas parameter "n" was found to increase with an increase in stress levels in creep tests and decrease with an increase in strain levels in relaxation tests. The temperature effect has not been considered in this study.

Data Availability Statement

Some or all of the data, models, or code generated or used during the study are available from the corresponding author by request, including Abaqus input and excel data files.

Acknowledgments

The funding of this research project was provided by the Natural Sciences and Engineering Research Council of Canada (NSERC) through its Collaborative Research and Development Grants, InnovateNL in the province of Newfoundland and Labrador, FortisBC Energy Inc., and WSP Canada. The financial support is gratefully acknowledged.

References

ASTM. 2003. *Standard test method for tensile properties of plastics*. ASTM D638-14. West Conshohocken, PA: ASTM.

Bilgin, Ö. 2014. "Modeling viscoelastic behavior of polyethylene pipe stresses." *J. Mater. Civ. Eng.* 26 (4): 676–683. https://doi.org/10.1061/(ASCE)MT.1943-5533.0000863.

Bilgin, Ö, H. E. Stewart, and T. D. O'Rourke. 2007. "Thermal and mechanical properties of polyethylene pipes." *J. Mater. Civ. Eng.* 19 (12): 1043–1052. https://doi.org/10.1061/(ASCE)0899-1561(2007)19:12(1043).

Brachman, R. W. I., I. D. Moore, and R. K. Rowe. 2000. "Local strain on a leachate collection pipe." *Can. J. Civ. Eng.* 27 (6): 1273–1285. https://doi.org/10.1139/l00-074.

Chehab, A. G. 2008. "Time dependent response of pulled-in-place HDPE pipes." Ph.D. thesis, Dept. of Civil Engineering, Queen's Univ.

Chehab, A. G., and I. D. Moore. 2006. "Constitutive model for high density polyethylene to capture strain reversal." In *Proc., Pipeline Division Specialty Conf. 2006*, 15419. Reston, VA: ASCE. https://doi.org/10.1061/40854(211)87.

Cholewa, J. A., R. W. I. Brachman, and I. D. Moore. 2011. "Axial stress-strain response of HDPE from whole pipes and coupons." *J. Mater. Civ. Eng.* 23 (10): 1377–1386. https://doi.org/10.1061/(ASCE)MT.1943-5533.0000320.

Chua, K. M., and R. L. Lytton. 1989. "Viscoelastic approach to modeling performance of buried pipes." *J. Transp. Eng.* 115 (3): 253–269. https://doi.org/10.1061/(ASCE)0733-947X(1989)115:3(253).

Colak, O. U., and N. Dusunceli. 2006. "Modeling viscoelastic and viscoplastic behavior of high density polyethylene." *J. Eng. Mater. Technol.* 128 (4): 572–578. https://doi.org/10.1115/1.2345449.

Dassault Systemes. 2013. *ABUQUS/CAE user's guide*. Providence, RI: Dassault Systemes Simulia Corp.

Dassault Systemes. 2015. *Abaqus user subroutines reference guide*. Providence, RI: Dassault Systemes Simulia Corp.

Debnath, S., and A. S. Dhar. 2019. "Assessment of stress intensity factor for buried cast iron pipeline using finite element analysis." In *Proc., 72nd Canadian Geotechnical Conf.* St. John's, NL, Canada: Canadian Geotechnical Society.

Duncan, J. M., and C. Y. Chang. 1970. "Nonlinear analysis of stress and strain in soils." *J. Soil Mech. Found. Div.* 96 (5): 1629–1653.

Hamouda, B. H., L. Laiarinandrasana, and R. Piques. 2007. "Viscoplastic behavior of a medium density polyethylene (MDPE): Constitutive equations based on double nonlinear deformation model." *Int. J. Plast.* 23 (8): 1307–1327. https://doi.org/10.1016/j.ijplas.2006.11.007.

Hashash, N. M. A. 1991. "Design and analysis of deeply buried polyethylene drainage pipes." Ph.D. thesis, Dept. of Civil Engineering, Univ. of Massachusetts at Amherst.

Kondner, R. L. 1963. "Hyperbolic stress-strain response: Cohesive soils." *J. Soil Mech. Found. Div.* 89 (1): 115–143.

Liu, H., M.A. Polak, and A. Penlidis. 2008. "A practical approach to modeling time-dependent nonlinear creep behavior of polyethylene for structural applications." *Polym. Eng. Sci.* 48 (1): 159–167. https://doi.org/10.1002/pen.20942.

May, D. L., A. P. Gordon, and D. S. Segletes. 2013. "The application of the Norton-Bailey law for creep prediction through power law regression." In Vol. 7 of *Proc., ASME Turbo Expo 2013: Turbine Technical Conference and Exposition*. San Antonio: ASME. https://doi.org/10.1115/GT2013-96008.

Moore, I. D. 1994. "Three-dimensional time dependent model for buried HDPE pipe." In *Proc., 8th Int. Conf. On Computer Methods and Advances in Geomechanics*, edited by H. J. Siriwardane and M. M. Zaman, 1515–1520. Rotterdam, Netherlands: A.A. Balkema.

Muntakim, A. H., A. S. Dhar, and A. Reza. 2018. "Modelling time dependent behavior of buried polyethylene pipes using Abaqus." In *Proc., 71st Canadian Geotechnical Conf.: GeoEdmonton 2019*. Edmonton, AB, Canada: Canadian Geotechnical Society.

Perzyna, P. 1966. "Fundamental problems in viscoplasticity." In *Advances in applied mechanics*, 243–377. Boston: Elsevier. https://doi.org/10.1016/S0065-2156(08)70009-7.

Popelar, C. F., C. H. Popelar, and V. H. Kenner. 1990. "Viscoelastic material characterization and modeling of polyethylene." *Polym. Eng. Sci.* 30 (10): 577–586. https://doi.org/10.1002/pen.760301004.

Powel, P. C. 1983. *Engineering with polymers*. Methuen, NY: Chapman and Hall.

Pulungan, D., A. Yudhanto, S. Goutham, G. Lubineau, R. Yaldiz, and W. Schijve. 2018. "Characterizing and modeling the pressure- and rate-dependent elastic-plastic-damage behaviors of polypropylene-based polymers." *Polym. Test.* 68 (Jul): 433–445. https://doi.org/10.1016/j.polymertesting.2018.02.024.

Siddiquee, M. S. A., and A. S. Dhar. 2015. "A novel elasto-viscoplastic model of high-density polyethylene material." *Geosynth. Int.* 22 (2): 173–182. https://doi.org/10.1680/gein.15.00003.

Suleiman, M. T., and B. J. Coree. 2004. "Constitutive model for high density polyethylene material: Systematic approach." *J. Mater. Civ. Eng.* 16 (6): 511–515. https://doi.org/10.1061/(ASCE)0899-1561(2004)16:6(511).

Swain, A., and P. Ghosh. 2019. "Determination of viscoelastic properties of soil and prediction of static and dynamic response." *Int. J. Geomech.* 19 (7): 04019072. https://doi.org/10.1061/(ASCE)GM.1943-5622.0001456.

Tobolsky, A. V. 1960. *Properties and structure of polymers*. New York: Wiley.

Weerasekara, L., and M. Rahman. 2019. "Framework for assessing integrity of natural gas distribution pipes in landslide areas." In *Proc., 72nd Canadian Geotechnical Conf.: Geo St. John's 2019*. St. John's, NL, Canada: Canadian Geotechnical Society.

Zhang, C., and I. D. Moore. 1997. "Nonlinear mechanical response of high-density polyethylene. Part II: Uniaxial constitutive modeling." *Polym. Eng. Sci.* 37 (2): 414–420. https://doi.org/10.1002/pen.11684.